Order–Disorder Transition of Low Molecular Weight Polystyrene-*block*-Polyisoprene. 1. SAXS Analysis of Two Characteristic Temperatures

Naoki Sakamoto and Takeji Hashimoto*

Division of Polymer Chemistry, Graduate School of Engineering, Kyoto University, Kyoto 606-01, Japan

Received February 23, 1995; Revised Manuscript Received June 27, 1995®

ABSTRACT: High-temperature-resolution small-angle X-ray scattering (SAXS) experiments were performed to elucidate the order–disorder transition at temperature T (T_{ODT}) and the crossover from the disordered state characterized by the Brazovskii-type non-mean-field theory to the disordered state characterized by the Leibler mean-field theory at T (T_{MF}) for low molecular weight polystyrene-*block*-polyisoprene copolymers having about equal block molecular weights. Across T_{ODT}, the inverse peak scattered intensity I_m^{-1} and the peak width σ_q clearly show a very sharp discontinuity, but the characteristic length D of the concentration fluctuations shows almost no change. The second-order scattering maximum existing below T_{ODT} definitely disappears above T_{ODT}, indicating that the spatial concentration fluctuation profile changes from a square-wave-type to a sinusoidal-wave-type profile upon increasing T through T_{ODT}. The crossover temperature T_{MF} is clearly identified from the changes in the temperature dependencies of I_m^{-1}, σ_q^2, and D with T: $\partial I_m^{-1}/\partial(1/T)$, $\partial\sigma_q^2/\partial(1/T)$, and $\partial D/\partial(1/T)$ all show a discontinuity at the same temperature T_{MF}. The temperature dependence D at $T > T_{MF}$ is explained by that of the radius of gyration R_{g0} of the unperturbed block copolymer chains, while that at $T < T_{MF}$ is much greater than that of R_{g0}.

I. Introduction

The order–disorder transition (ODT) of block copolymer melts has been extensively studied since Leibler's pioneering theory,[1] and some initial experimental results[2–7] have been reported. Some important pieces of evidence have recently been elucidated for block copolymer melts having relatively weak segregation power χN, where χ is the Flory–Huggins segmental interaction parameter and N is the total degree of polymerization of the block copolymers. These pieces of evidence, as will be described below, were obtained in fragments: some limited number of results were obtained on different block copolymers, and various pieces of information have not been systematically obtained on the same block copolymer. In this series of studies we aim to obtain systematically the various pieces of information, extractable from scattering methods, on the same block copolymer, on block copolymers having different molecular weights, or on block copolymer solutions having different polymer concentrations.

In this work we focus on the physical quantities obtainable from small-angle X-ray scattering (SAXS) and small-angle neutron scattering (SANS): the scattering peak intensity I_m, the scattering vector q_m, which gives the maximum scattered intensity or the characteristic length,

$$D \equiv 2\pi/q_m \tag{1}$$

the half-width at half-maximum σ_q of the first-order scattering peak, and the second-order scattering maximum or shoulder. Existence of the second-order maximum is physically important because it implies that spatial concentration fluctuations of block copolymer segments deviate from sinusoidal-wave-type fluctuations, as in the case of square-wave-type fluctuations.

Conventionally,[3–5,7–9] ODTs have been determined from the scattering experiments on the basis of Leibler's Landau type mean-field theory.[1] The theory predicts that the scattered intensity $I(q)$ at scattering vector q in the disordered state is given by

$$[I(q)/N]^{-1} \sim F(q) - 2\chi N \tag{2}$$

The quantity q is defined by

$$q = (4\pi/\lambda)\sin(\theta/2) \tag{3}$$

where λ and θ are the wavelength and scattering angle in the medium. $F(q)$ is a function which depends on the radius of gyration R_g and the composition f of a block copolymer. $F(q)$ has a minimum and hence $I(q)$ has a maximum intensity I_m at $q = q_m$, the value of which does not explicitly depend on χ and hence on temperature T. However, it depends weakly on T through the temperature dependence of R_g. Thus in the disordered state, I_m^{-1} should change linearly with $1/T$ as schematically shown in Figure 1a in the temperature range $T > T_{ODT,MF}$, if χ changes with T according to

$$\chi = A + B/T \tag{4}$$

D, defined by eq 1, should also change linearly with $1/T$ in the narrow temperature range of $T > T_{ODT,MF}$, because $D(T) \propto R_g(T)$. A deviation of D or I_m^{-1} from linearity at $T \leq T_{ODT,MF}$ was considered to be an onset of ordering. We define here the ODT temperature thus determined based on the mean-field theory as a mean-field ODT temperature $T_{ODT,MF}$ for the sake of convenience.

Bates et al.[10] reported an important finding on the ODT of a PEP–PEE block copolymer: the plot of I_m^{-1} vs T^{-1} shows a discontinuous change at a particular temperature, designated here T_{ODT} for the sake of convenience. Surprisingly, D shows no change at T_{ODT}, as schematically shown in Figure 1b. The temperature dependence of D was reported to be identical to that of the R_g of the block copolymer in the unperturbed state (R_{g0}) over the whole temperature range covered by their experiment, the behavior of which is very different from that shown in Figure 1a. This is one of the research

® Abstract published in *Advance ACS Abstracts,* September 1, 1995.

0024-9297/95/2228-6825$09.00/0

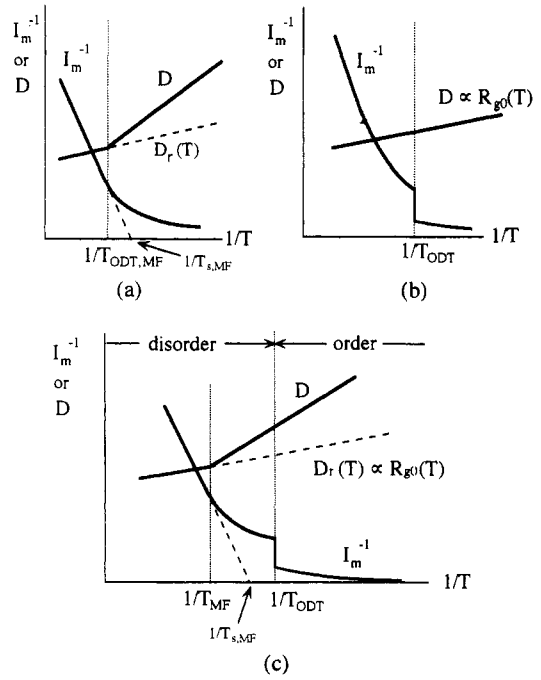

Figure 1. Temperature dependence of the characteristic scattering parameters, i.e., the inverse maximum intensity I_m^{-1} and the characteristic length D determined from the scattering vector q_m at the first-order scattering maximum: (a) a conventional view, (b) a new view, and (c) a unified view found in this work.

items that we address in this work (**item 1**). Since the reported discontinuity of I_m at T_{ODT} was small, the scattering data alone may overlook the discontinuity at T_{ODT}. The ODT independently assessed by the temperature dependence of the low-frequency shear modulus of the same sample as well as the theoretical analyses given confirmed the discontinuity of I_m^{-1} at T_{ODT}. This discontinuity and the nonlinear change of I_m^{-1} with T^{-1} were ascribed to the thermal fluctuation effect[11] (the Brazovskii effect[12]). They reported that even in the disordered state, $I(q)$ near T_{ODT} shows the second-order shoulder at $q \cong 2q_m$, and the corresponding scaled structure factor at $q/q_m \leq 3$ is nearly identical to that of the phase-separated domain structure in the PEP/PEE blend *at the late stage spinodal decomposition*.[13] This implies that the corresponding spatial concentration fluctuations are of a square-wave type, against our intuition that the fluctuations in the disordered state are of a sinusoidal-wave type. We wish to confirm this surprising observation in this work, because this important point has been apparently overlooked in the literature. This point also is a research item to be addressed in this work (**item 2**).

For polystyrene-*block*-polyisoprene (SI) and polystyrene-*block*-polybutadiene (SB) diblock copolymers, however, the discontinuity of I_m^{-1} as shown in Figure 1b has not been found until quite recently where Stühn et al.,[14] Wolff et al.,[15] Hashimoto et al.,[16] and Floudas et al.[17] found the discontinuity in I_m^{-1} vs T^{-1}. Their results may imply that the earlier works[2-5,9] which led to determination of $T_{ODT,MF}$ overlooked the ODT, which presumably existed at T much lower than $T_{ODT,MF}$ or existed in between two successive temperatures, the interval of which were too wide compared with the sharpness of the ODT phenomenon. Recent work by Winey et al.[18] could not find a sharp discontinuous nature of the ODT. Their results[2-5,9] indicated either explicitly or implicitly that at high enough temperatures in the disordered state above T_{ODT}, I_m^{-1} linearly changes with T^{-1} in accord with the mean-field theory. Thus we may propose that the temperature $T_{ODT,MF}$ corresponds to a crossover temperature T_{MF} above which I_m^{-1} vs T^{-1} can be *approximately* described by the mean-field theory and the T_{ODT} at which the discontinuity occurs to be the true ODT temperature T_{ODT}, as shown in Figure 1c. T_{MF} is regarded to be the crossover temperature from the mean-field-type to the non-mean-field-type disordered state. This existence of the two characteristic temperatures and variations of I_m^{-1} and D at these temperatures as shown in Figure 1c have not yet been fully analyzed in the literature. Moreover, the relation between T_{MF} and T_{ODT} has not been experimentally analyzed. This may be partly because it is difficult for us to define T_{MF} rigorously because of the reasons described below and partly because T_{MF} exists at relatively high temperatures where the scattering intensity is very weak. In this paper we discuss this relation between the two characteristic temperatures T_{MF} and T_{ODT} (**item 3**).

It is important to note that it is not possible to define T_{MF} from a rigorous theoretical point of view, because the mean-field behavior is achieved only asymptotically. Nevertheless we believe it is useful for us to define it from an experimental point of view: we can *operationally* define T_{MF} such that above T_{MF} we can practically analyze, to a good approximation, our experimental data based on the mean-field theory.

It is important to investigate the behavior of I_m^{-1} vs T^{-1} simultaneously with the behavior of D or q_m. The results reported by Stühn et al.,[14] Wolff et al.,[15] and Hashimoto et al.[16] are different from those reported by Bates et al.:[10] for the SI and SB block copolymers, the temperature dependence of D or $1/q_m$ is not identical to that of R_{g0} as shown in Figure 1b. Stühn et al.[14] reported "q_m shifts continuously from a value given by the unperturbed chain dimension $R_{g0}(T)$ by 15% to smaller values" with increasing T^{-1}. We may speculate that they observed D in the temperature range satisfying $1/T > 1/T_{MF}$ in Figure 1c. Wolff et al.[15] made no comments on the relation between q_m and $R_{g0}(T)$. Floudas et al.[17] gave no analysis of D for their diblock copolymer. Hashimoto et al.[16] reported that the temperature dependence of D at $T > T_{ODT}$ is larger than that of $R_{g0}(T)$. However, they could not approach the temperature range of $T > T_{MF}$ with their SI block copolymer. They speculated that this temperature range should exist above the highest temperature they could approach. Stühn et al.[14] reported a slight discontinuous increase of D at T_{ODT}, but Hashimoto et al.[16] reported no change of D at T_{ODT} for the lamellar-forming block copolymers, as in the case of Bates et al.[10] No comments were given by Wolff et al.[15] and Floudas et al.[17] on this point. Thus the temperature dependence of D or q_m should be further reexamined in parallel with that of I_m^{-1} (item 1 given earlier in this paper) systematically for the same block copolymers.

The second-order maximum or shoulder of the structure factor at $T > T_{ODT}$ has not been reported for the SI and SB diblock copolymers except in the work by Hashimoto et al.,[16] who reported no second-order maximum or shoulder at $T > T_{ODT}$. This point also will be reexamined in this work for other SI block copolymers (item 2).

After this paper was submitted, a new paper by Rosedale et al.[19] appeared. Since that paper deals with the ODT for the diblock copolymers PE−PEE-6H, PEP−

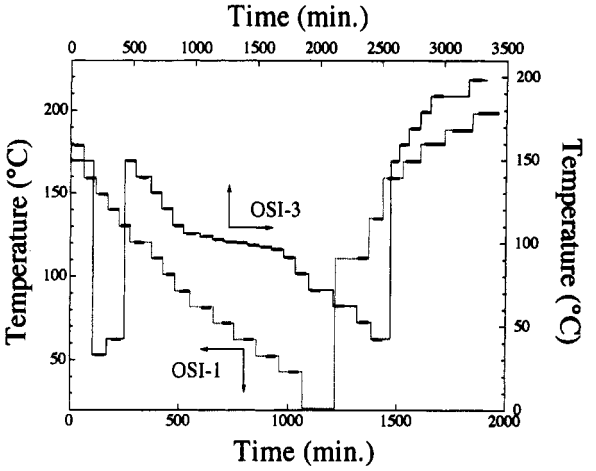

Figure 2. Thermal programs given in the SAXS experiments for OSI-1 and OSI-3.

Table 1. Characteristics of SI Diblock Copolymers Used in This Work

polymer	vol fraction of PS	M_n	M_w/M_n	T_{ODT}/°C	T_{MF}/°C
OSI-1	0.54	1.2×10^4	1.02	below 40	135
OSI-3	0.45	1.5×10^4	1.02	100	169

PEE-14H and PE–PEE-8H as observed by small-angle neutron scattering (SANS), it may be appropriate to comment briefly on their new results here. First, it was confirmed again that D shows no change at T_{ODT} determined with the benefit of rheology for PE–PEP-6H, although this continuity of D at T_{ODT} was not directly confirmed for the other two polymers (item 1). Second, a brief comment was given on the second-order maximum or shoulder at T above T_{ODT} (item 2); as PE–PEP-6H is heated toward the ODT, the number of Bragg refractions decrease to just one. Thus existence of the second-order maximum at T above T_{ODT} was denied clearly at least for PE–PEP-6H. Third, the temperature dependencies of D for all three samples were found to be different from that for PEP–PEE previously reported:[10] for each sample studied, dD/dT increases around the crossover temperature to mean-field behavior defined as T_x, instead of the previous results of $dD/dT = dR_{g0}/dT$ at all the temperatures covered.[10] T_x may correspond to T_{MF} shown in Figure 1c, and D vs T^{-1} seems similar to that shown in Figure 1c, except for the fact that even at $T > T_x$, dD/dT was found to be greater than dR_{g0}/dT for each sample reported.

In the present paper we focus on the exploration of the three research items described above for a better understanding of the ODT phenomenon of low molecular weight symmetric block copolymers of SI and SB.

II. Experimental Methods

Two kinds of SI diblock copolymers, OSI-1 and OSI-3, were prepared by living anionic polymerization with *sec*-butyllithium as initiator and cyclohexane as a solvent according to the standard method. Their molecular characteristics are listed in Table 1.

SAXS was measured *in situ* at each temperature with the SAXS apparatus described elsewhere.[20] The sample temperature was controlled with an accuracy of ±0.03 °C with a new temperature enclosure constructed in our laboratory. The sample was put in an evacuated chamber to reduce possible thermal degradation.

In Figure 2 we present the temperature programs for OSI-1 and OSI-3 used for the SAXS data collection presented in this paper. For OSI-3, the SAXS measurements were done at 1 deg temperature increments near the ODT temperature. At each measuring temperature the samples were held for about 30 min before measurement with a measuring time of about 60 min.

The SAXS profiles were desmeared for slit-width and slit-height smearings and corrected for absorption, air scattering, and thermal diffuse scattering as described elsewhere.[20]

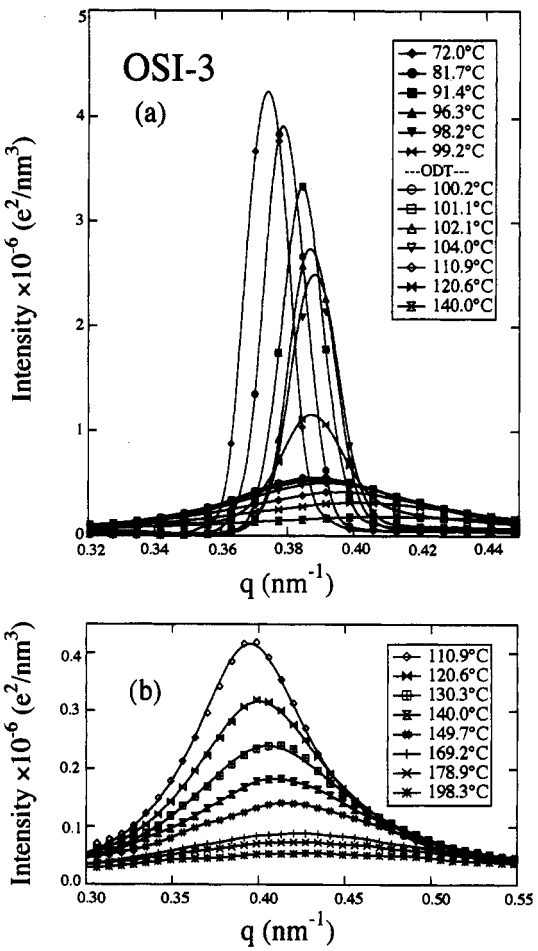

Figure 3. Temperature dependence of the SAXS profiles for OSI-3. Parts a and b highlight, respectively, the change in the profiles across the ODT and that in the disordered state.

III. Experimental Results

Figure 3 shows the corrected SAXS profiles from OSI-3 taken *in situ* at various temperatures according to the thermal program shown in Figure 2. A sharp and remarkable change of the profiles is clearly discerned at temperatures between 99.2 and 100.2 °C in part a. This discontinuous change of the SAXS profile enables a clear-cut determination of the ODT temperature (T_{ODT}) of this block copolymer. T_{ODT} thus determined is $99.2 < T_{ODT} < 100.2$ °C. The profile continuously changes at $T > T_{ODT}$ as shown in part b. Figure 4 shows the corrected SAXS profiles from OSI-1 taken *in situ* at various temperatures according to the thermal program shown in Figure 2. We observe a continuous change of the profiles in terms of peak width and peak position over the temperature range covered in this work. Judging from the peak width, it is reasonable to assume that the OSI-1 block copolymer is in the disordered state in this temperature range. We will analyze the SAXS profiles shown in Figures 3 and 4 in the next section.

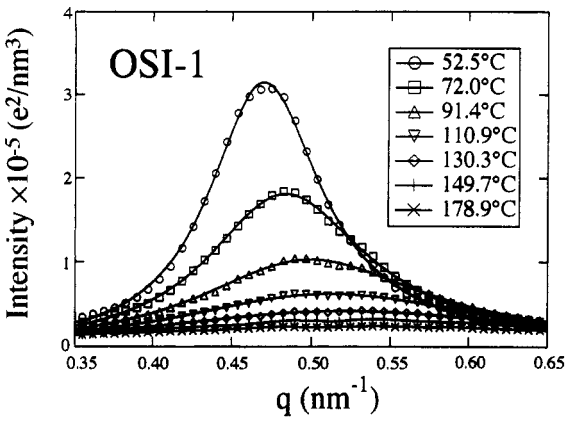

Figure 4. Temperature dependence of the SAXS profiles for OSI-1.

IV. Analysis and Discussion

A. Discontinuity at the ODT Temperature. The scattering function $I(q)$ in eq 2 can be rewritten as follows:

$$I(q) \sim I_m/[1 + (q - q_m)^2\xi^2] \quad (5)$$

at q close to q_m, where ξ is the thermal correlation length for the concentration fluctuations in the disordered state. We define σ_q as the half-width at half-maximum of $I(q)$ for the scattering from the disordered state. Then σ_q is equal to $1/\xi$ and thus the Landau mean-field theory predicts that

$$\sigma_q^2 = 1/\xi^2 \sim (1/R_{g0}^2)(\chi_s - \chi)/\chi_s \sim \frac{1}{N}(\chi_s - \chi)/\chi_s \sim 1/T_s - 1/T \quad (6)$$

where χ_s is the χ-value at the mean-field spinodal temperature T_s. Note that we used eq 4 for the temperature dependence of χ and $\chi_s \sim 1/N$. From eqs 2 and 4, it follows that

$$(I_m/N)^{-1} \equiv [I(q_m)/N]^{-1} \sim F(q_m) - 2\chi N = 2(\chi_s - \chi)N \sim (1/T_s - 1/T)N \quad (7)$$

Thus σ_q^2 is not a parameter independent of I_m^{-1}. However, σ_q^2 is a very useful parameter from an experimental point of view, because it is free from error in the absolute intensity measurement. This quantity was found to be very sensitive to the ODT.

Figure 5 shows I_m^{-1} and σ_q^2 plotted as a function of $1/T$ for OSI-3. As expected, both I_m^{-1} and σ_q^2 have a similar temperature dependence, especially at $T \geq T_{ODT}$. I_m^{-1} and σ_q^2 show a sharp discontinuous change in the narrow temperature range between 99.2 (point 3 in the inset) and 100.2 °C (point 4). We can assess that T_{ODT} is 99.2 < T_{ODT} < 100.2 °C and the disordered state exists at $T \geq T_{ODT}$. At $T \leq 98.2$ °C, the second-order SAXS maximum exists as will be shown later in Figure 10, implying that the system is clearly in an ordered state having the lamellar microdomain morphology.

Since the characteristic parameters I_m^{-1} and σ_q^2 in the narrow temperature range where the ODT occurs have never been closely investigated, we will describe them briefly below. The values I_m^{-1} and σ_q^2 at $T = 99.2$ °C (point 3 in the inset) are in between those at 100.2 and 98.2 °C (point 2 in the inset), even after annealing at this temperature (for ca. 0.5 h). The SAXS profile at $T = 99.2$ °C, $I(q:T=99.2\ °C)$, can be approximately expressed in terms of a weighted average of the profiles

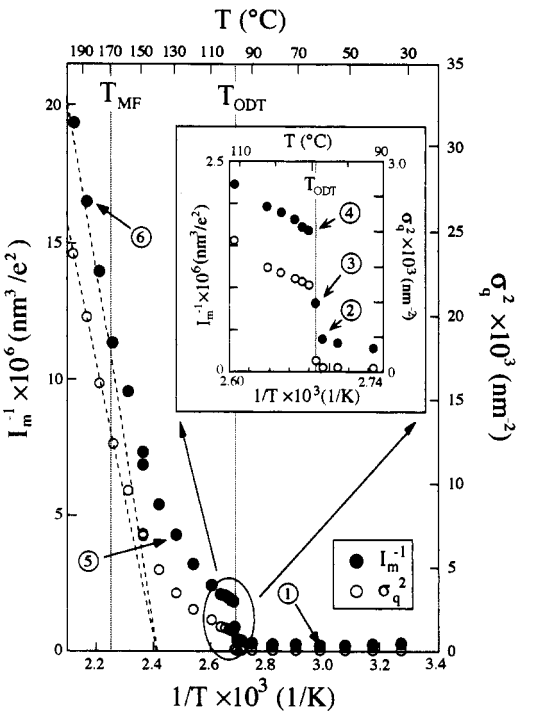

Figure 5. I_m^{-1} and σ_q^2 (square of the half-width at half-maximum of the first-order SAXS maximum) plotted as a function of $1/T$ for OSI-3. The inset at the upper right corner of the figure shows a close up of I_m^{-1} and σ_q^2 vs $1/T$ near T_{ODT}. The two characteristic temperatures T_{MF} and T_{ODT} are shown, and $T_{MF} - T_{ODT} \cong 70$ °C for this polymer. The number corresponds to the scattering profile shown later in Figure 10.

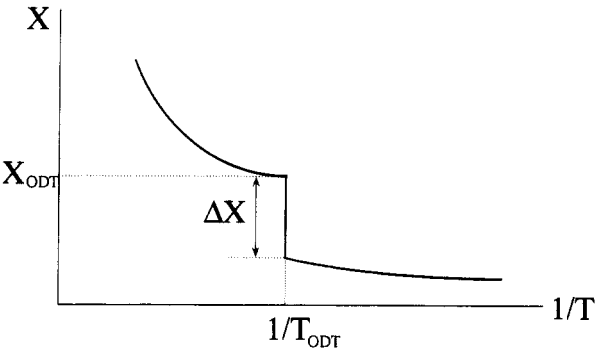

Figure 6. Definition of discontinuity ΔX in the temperature dependence of a quantity X at T_{ODT}. X_{ODT} is defined as the value of X at the limit of $T \to T_{ODT}$ in the disordered side.

at $T = 100.2$ °C, $I(q:T=100.2\ °C)$, and at 98.2 °C, $I(q:T=98.2\ °C)$, i.e.,

$$I(q:T=99.2\ °C) \cong X_{dis}\, I(q:T=100.2\ °C) + (1 - X_{dis})I(q:T=98.2\ °C) \quad (8)$$

with $X_{dis} \cong 0.35$. Thus we tentatively assume that the ordered phase coexists with the disordered phase in a very narrow temperature range around T_{ODT}, presumably due to a small polydispersity effect. This coexistence may be also ascribed to a metastability of the system at this temperature. A further annealing effect should be studied in the future.

It is worthwhile to study the amount of discontinuity of a quantity X at T_{ODT}, where X is either I_m^{-1} or σ_q^2, since no such attempt has been made so far and the discontinuity is closely related to the nature of the ODT. For this purpose we may be able to deal with a dimensionless quantity $\Delta X/X_{ODT}$ as defined in Figure 6, where ΔX is the amount of discontinuity of X, and

Table 2. Comparisons of the Reduced Discontinuities at T_{ODT} Observed for Various Diblock Copolymers

	$\Delta I_m^{-1}/I_{m,ODT}^{-1}$	$\Delta\sigma_q^2/\sigma_{q,ODT}^2$	block copolymers A–B	N_A[a]	N_B[b]	ref
Bates et al.	0.19		PEP–PEE	564	462	10
Stühn et al.	0.08	0.74	PS–PI	71	122	14
Wolff et al.	0.74		PS–PB	108	121	15
Floudas et al.	0.32	0.65	PS–PI	65	81	17
Hashimoto et al.	0.70	0.85	PS–PI	80	123	16[c]
this work (OSI-3)	0.71	0.94	PS–PI	67	118	

[a] Degree of polymerization of PEP or PS. [b] Degree of polymerization of PEE, PI, or PB. [c] The discontinuities in this row were evaluated after desmearing the SAXS profiles.

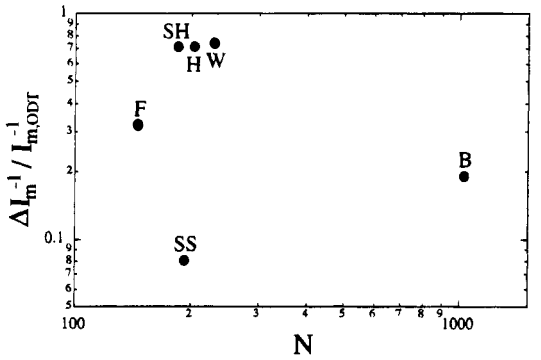

Figure 7. Comparisons of the reduced discontinuity $\Delta I_m^{-1}/I_{m,ODT}^{-1}$ reported by the number of groups shown in Table 2. F, SH, SS, H, W, and B refer to Floudas et al., Sakamoto et al. (this work), Stühn et al., Hashimoto et al., Wolff et al., and Bates et al., respectively (see Table 2).

X_{ODT} is the value X in the disordered state very close to T_{ODT}. Table 2 and Figure 7 compare the reduced discontinuities of $\Delta I_m^{-1}/I_{m,ODT}^{-1}$ and $\Delta\sigma_q^2/\sigma_{q,ODT}^2$. Currently, it seems difficult to draw definite conclusions from this table and figure, because of the scattering in the data, which may be due to a difference in the composition $f = N_A/(N_A + N_B)$ as well as that in the thermal history such as heating and cooling rates etc. in each experiment cited. Nevertheless it may be safe to expect that $\Delta I_m^{-1}/I_{m,ODT}^{-1}$ tends to decrease with increasing N except the data point (SS) obtained by Stühn et al. This trend is consistent with the theoretical prediction.[11] The quantitative analysis of these quantities deserves future work.

B. Crossover between Brazovskii Behavior and Mean-Field Behavior at T_{MF} in the Disordered Region and the Relationship between T_{MF} and T_{ODT}. Although there is a problem in rigorously defining the crossover temperature T_{MF} as discussed in section I, we operationally try to identify T_{MF} in this section from the temperature dependencies of I_m^{-1}, σ_q^2, and D.

At sufficiently high temperature, I_m^{-1} vs $1/T$ and σ_q^2 vs $1/T$ in OSI-3 show *approximately* linear relationships, as predicted by eqs 6 and 7. Upon further lowering T or increasing $1/T$, both I_m^{-1} and σ_q^2 start to clearly deviate from the linear relationship, showing a downward convex curvature, approximately at the same temperature T_{MF}. This deviation from the mean-field behavior at $T_{ODT} \leq T \leq T_{MF}$ is interpreted as the thermal fluctuation effect (the Brazovskii effect[12]) elaborated by Fredrickson and Helfand.[11] The thermal fluctuations shift the temperature below which ordering starts from the mean-field spinodal temperature $T_{s,MF}$ (≅140 °C) down to T_{ODT} (≅100 °C). As a consequence, both I_m^{-1} and σ_q^2 at $T_{s,MF} < T < T_{MF}$ in real systems become larger than the values predicted by the mean-field theory: the random thermal force tends to suppress the concentration fluctuations (the Brazovskii effect). In other words, the concentration fluctuations and thermal correlation length in a real system are smaller than the values predicted by the mean-field theory.

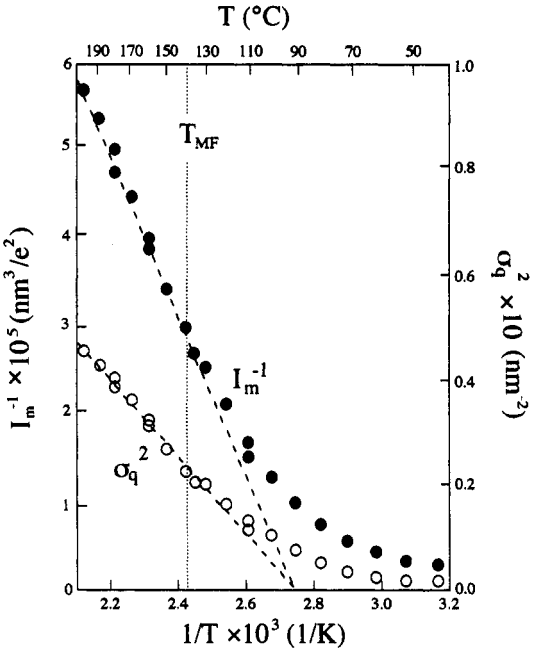

Figure 8. I_m^{-1} and σ_q^2 plotted as a function of $1/T$ for OSI-1.

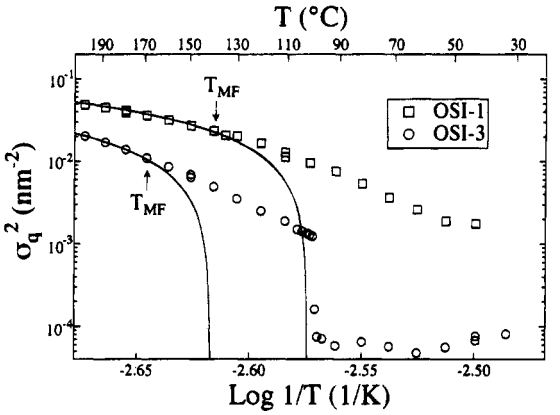

Figure 9. Comparison of σ_q^2 vs $1/T$ for OSI-1 and OSI-3 in the double-logarithmic scale.

Since the mean-field regime covered in the block copolymer OSI-3 is relatively narrow (i.e., 170 ≲ T ≲ 198 °C), we checked the crossover behavior by using OSI-1 having a molecular weight and T_{MF} lower than those of OSI-3. The results for OSI-1 are shown in Figure 8. In this polymer T_{ODT} is not clearly discerned, probably because T_{ODT} is lower than the observed temperature range or the glass transition temperature of OSI-1. Hence we can only observe the crossover temperature T_{MF}. A comparison of the results shown in Figures 5 and 8 clearly indicates that the temperature range for the mean-field behavior in OSI-1 is much wider than that in OSI-3. Figure 9 compares the σ_q^2 vs $1/T$ relationships for the two polymers in double-logarithmic scale. The solid lines in the figure present the mean-field behavior predicted from eq 6 with $T_{s,MF}$ = 92 and 140 °C for OSI-1 and OSI-3, respectively. This figure clearly suggests that OSI-1 is in the disordered state over the whole temperature range covered. The shifts of T_{MF} and T_{ODT} with molecular weight are also

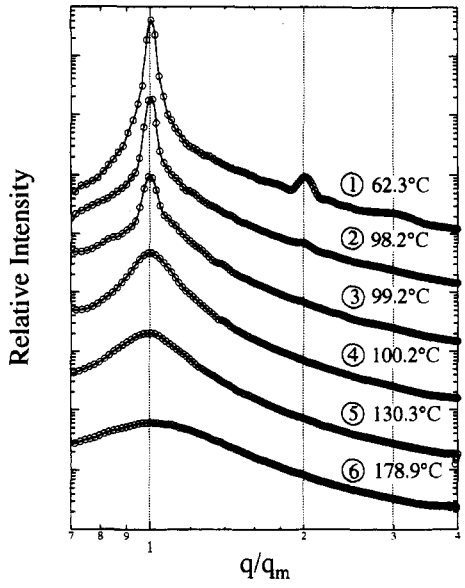

Figure 10. SAXS intensity distributions against a reduced scattering vector q/q_m in the double-logarithmic scale from OSI-3 at the specified temperatures (see Figure 5 for the temperatures examined here).

clearly presented in the figure.

At this stage we try to make a qualitative comparison of the reported results on the quantity $\Delta(1/T)_{ODT}$, defined by

$$\Delta(1/T)_{ODT} \equiv 1/T_{ODT} - 1/T_{MF} \quad (9)$$

Although this quantity was not discussed in depth in earlier works, we can estimate $\Delta(1/T)_{ODT} \cong 2.8 \times 10^{-4}$ K^{-1} from the work by Stühn et al. (estimated from Figure 3 of ref 14) and 4.2×10^{-4} K^{-1} from the work by Wolff et al. (estimated from Figure 3 of ref 15). Our results for OSI-3 show $\Delta(1/T)_{ODT} \cong 4.4 \times 10^{-4}$, close to the results by Wolff et al.

The temperature gap $\Delta(1/T)_{ODT}$ and the crossover behavior will be further discussed in conjunction with the temperature dependence of D in section D later. However, before the discussion, we will closely examine the change in the second-order maximum or shoulder of the structure factor across T_{ODT}.

C. Second-Order Maximum or Shoulder. We now closely investigate the existence of the second-order maximum or shoulder in the disordered state near the ODT. This important issue has not been discussed so far on SI and SB diblock copolymers. The scattering data reported so far appear to be not good enough to discuss this important issue. We believe this issue is very important because it is also associated with the effect of critical concentration fluctuations on rheology.

Figure 10 shows the scattering intensity from OSI-3 plotted as a function of a reduced scattering vector q/q_m in double-logarithmic scale. Far below T_{ODT}, e.g., at 62.3 °C, the scattering maxima are clearly seen up to the third order at the positions of $q/q_m = 1$, 2, and 3, indicating formation of lamellar microdomains with a long-range spatial order. At 98.2 °C, very close to T_{ODT}, the third-order maximum disappears but the second-order maximum remains, indicating that the interface between coexisting microdomains becomes broad; thus the third-order harmonics of the dominant Fourier mode of the concentration fluctuations disappear. At 99.2 °C, where the system is in the ordered state very close to the ODT, the second-order maximum disappears. Moreover, the scattering profile at $q/q_m \gtrsim 2$ is almost identical

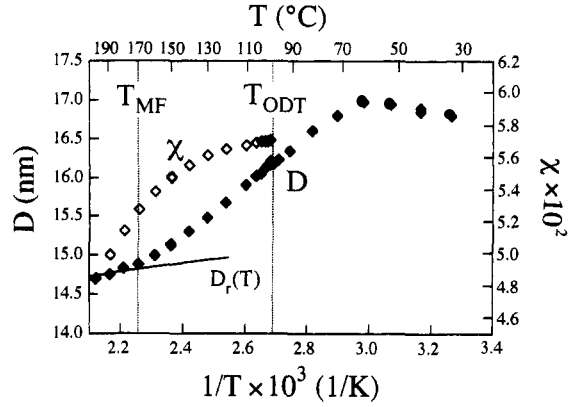

Figure 11. Temperature dependencies of D, $D_r(T)$, and χ in OSI-3.

to those at 130.3 and 178.9 °C, far above the ODT. Although not shown here, all the SAXS profiles from OSI-1 in the disordered state show only the first-order scattering maximum, consistent with the results for OSI-3 in the disordered state.

Thus we can clearly conclude that the second-order maximum disappears in the disordered state. Hence the spatial concentration profile in the disordered state is a sinusoidal-wave-type profile rather than a square-wave-type profile, consistent with our previous result[16] but not consistent with the report by Bates et al.[10] If we may assume, as a possibility, that the ODT reported by Bates et al.[10] corresponds to an order–order transition, we may be able to resolve this discrepancy observed in the PEP–PEE and SI block copolymers, although the possibility does not seem to be high. If this is the case, an enhancement of the low-frequency shear moduli observed in the PEP–PEE specimen[10] may be then accounted for in terms of ordered microdomains (such as perforated lamellae, for example) with defects. The defects, which are continuous in three-dimensional space, may give rise to the liquid-like response in the low-frequency rheological behavior. If this is the case, a serious problem arises as to an assessment of a T_{ODT} for this system. Their SANS results obtained with the shear-oriented lamellae show that when the temperature was raised through the ODT, the pattern changed from the diffraction spots oriented parallel to the lamellar normals to the azimuthally symmetric pattern, which was taken as a piece of evidence showing the transition from lamellae directly to the disordered liquid. However, a distorted bicontinuous phase might also show the azimuthally symmetric pattern. Another possibility may be the coexistence of the ordered phase and the disordered phase at a very narrow temperature range near the ODT due to a small polydispersity in molecular weight. In this case, the ordered phase may give rise to the second-order maximum or shoulder. In any case, clarification of these points deserves future work.

D. Temperature Dependence of the Characteristic Length D. Figures 11 and 12 show the characteristic length D determined from q_m (eq 1) as a function of $1/T$. The figures include the χ-values estimated from the best fit of the SAXS profiles with the theoretical profile given by Leibler's mean-field theory (eq 2) as well as the temperature dependence of $D_r(T)$ defined by eq 10.

$$D_r(T) = [R_{g0}(T)/R_{g0}(T_r)]D(T_r) \quad (10)$$

Here $D_r(T)$ gives the temperature dependence of D as

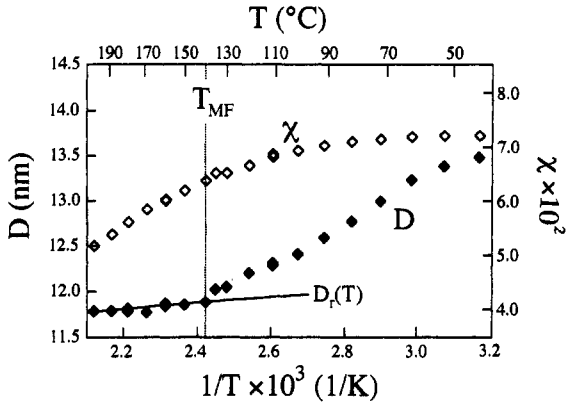

Figure 12. Temperature dependencies of D, $D_r(T)$, and χ in OSI-1.

predicted from the temperature dependence of the unperturbed chain dimension $R_{g0}(T)$, and T_r is a reference temperature, taken at 188.6 and 178.8 °C for OSI-3 and OSI-1, respectively. $R_{g0}(T)$ is expressed by

$$R_{g0}(T) = R_{g0}(T_r)\exp[(T - T_r)\kappa/2] \quad (11)$$

κ is the thermal expansivity of the polymer, defined by $\kappa \equiv d[\ln R_{g0}(T)^2]/dT$. In the case of diblock copolymer, κ is given by eq 12 by using κ_i and N_i, which denote the thermal expansivity and the number-average degree of polymerization of the ith segment, respectively.

$$\kappa = \frac{N_1}{N_1 + N_2}\kappa_1 + \frac{N_2}{N_1 + N_2}\kappa_2 \quad (12)$$

With the literature values of κ, -1.1×10^{-3} K^{-1} [21] for polystyrene and 0 K^{-1} for 1,4-polyisoprene, we obtained $\kappa = -4.0 \times 10^{-4}$ K^{-1} and $\kappa = -4.6 \times 10^{-4}$ K^{-1} for OSI-3 and OSI-1, respectively. The temperature dependence of χ will be described in section E later.

The figures include the two characteristic temperatures T_{MF} and T_{ODT} as determined in sections A and B. It should be noted that almost no change in D occurs at T_{ODT}, consistent with earlier reports by Bates et al.[10] and Hashimoto et al.[16] and a new report of Rosedale et al. on PE–PEP-6H[19] but inconsistent with the report by Stühn et al.[14] No comments were given by Wolff et al.[15] and Floudas et al.[17] So far we are not able to reproduce the observation made by Stühn et al. on the slight discontinuous increase of D at T_{ODT}, at least for the symmetric block copolymers.

There occurs a remarkable change in the temperature dependence of D at T_{MF}: above T_{MF} the temperature dependence of D can be *approximately* described by the temperature dependence of $R_{g0}(T)$, as shown by $D(T) \sim D_r(T)$ and, below T_{MF}, D increases with $1/T$ much more than $D_r(T)$. This change in $\partial D/\partial(1/T)$ at T_{MF} seems to be consistent with earlier reports by Stühn et al.[14] and Wolff et al.,[15] although Stühn et al. reported a continuous change in $\partial D/\partial(1/T)$ with $1/T$ and Wolff et al. did not compare $1/q_m$ with $R_{g0}(T)$ at $T > T_{MF}$. This change, however, is inconsistent with the result reported by Bates et al.[10] (although their data in Figure 10 in ref 10 might show a slight change in $\partial D/\partial(1/T)$ at $T \cong 151.6$ °C or 424.6 K). A similar trend is observed in OSI-1 at T_{MF}: $\partial D/\partial(1/T) \cong \partial R_{g0}/\partial(1/T)$ at $T > T_{MF}$ and $\partial D/\partial(1/T) > \partial R_{g0}/\partial(1/T)$ at $T < T_{MF}$. This change in $\partial D/\partial(1/T)$ at $T > T_{ODT}$ seems to be consistent with some theoretical predictions (the chain fluctuation effect[23] and the fluctuation-induced deviations from Gaussian statistics[24]).

The change of $\partial D/\partial(1/T)$ at $T = T_{MF}$ appears to be consistent with the new results reported by Rosedale

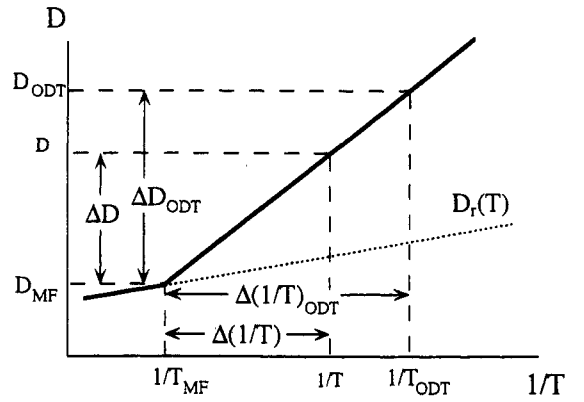

Figure 13. Schematic diagram showing D as a function of $1/T$ and definitions of various quantities such as ΔD, ΔD_{ODT}, $\Delta(1/T)$, and $\Delta(1/T)_{ODT}$.

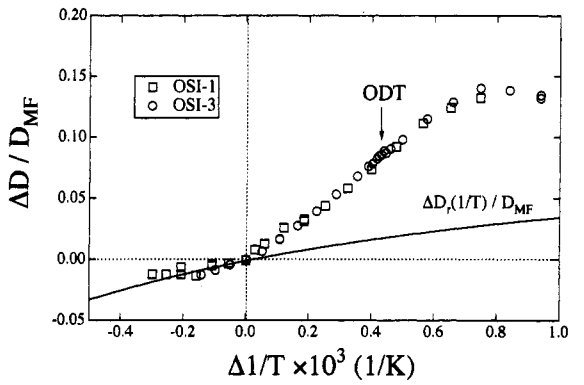

Figure 14. Temperature dependencies of $\Delta D/D_{MF}$ and $\Delta D_r/D_{MF}$ (solid line) in OSI-1 and OSI-3. The arrow indicates $\Delta(1/T)_{ODT}$ for OSI-3.

et al. on PE–PEP-6H, PEP–PEE-14H, and PE–PEE-18H:[19] they reported $\partial \ln q^*/\partial T$ changed at $T = T_x$, where q^* corresponds to q_m in this paper and T_x is the crossover temperature to the mean-field like behavior. However, there remains one important difference: our results show that $\partial D/\partial(1/T) \cong \partial R_{g0}/\partial(1/T)$ at $T > T_{MF}$, while their results show $\partial D/\partial(1/T)$ is bigger than $\partial R_{g0}/\partial(1/T)$ even at $T > T_x$ for all three block copolymers studied. Thus this point deserves further investigation for polystyrene-*block*-polyisoprene, polystyrene-*block*-polybutadiene, etc.

Figure 13 schematically summarizes the temperature dependence of D and the various quantities we will define hereafter for the sake of convenience.

$$\Delta D \equiv D(1/T) - D_{MF}, \quad D_{MF} \equiv D(1/T_{MF}) \quad (13)$$

$$\Delta D_{ODT} = D_{ODT} - D_{MF}, \quad D_{ODT} \equiv D(1/T_{ODT}) \quad (14)$$

$$\Delta(1/T) = 1/T - 1/T_{MF} \quad (15)$$

Our preliminary results show $\Delta(1/T)_{ODT}$ (eq 9) and ΔD_{ODT} are generally functions of the molecular weights and concentrations (when solvent is added) of diblock copolymers with a given composition f. Generally, $\partial D/\partial(1/T)$ changes slightly even at T_{ODT}, although the change is small compared with that at T_{MF} and the change is negligible for the particular block copolymer OSI-3 studied here.

Figure 14 shows a plot of the reduced quantity $\Delta D/D_{MF}$, the change of D relative to D_{MF}, as a function of $\Delta(1/T)$, the relative shift of $1/T$ with $1/T_{MF}$. The arrow indicates the T_{ODT} for OSI-3. The solid line indicates the change of $\Delta D_r/D_{MF}$, where $\Delta D_r \equiv D_r(1/T) - D_{MF}$. Our

preliminary results tend to show that $\Delta D/D_{MF}$ depends on N at $T < T_{MF}$ but is independent of N at $T > T_{MF}$, though this N dependence is too small to be clearly discernible with this scale for OSI-1 and -3. Thus $\Delta(1/T)_{ODT}$ and ΔD_{ODT} appear to be a function of N. Further work along this line needs to be done in the future.

E. Estimation of the χ-Parameter. The χ-parameters were estimated by analyzing the scattering profiles from the disordered melts on the basis of Leibler's mean-field theory (eq 2) modified for the effects of molecular weight polydispersity and asymmetry in segmental volume[22] (see Appendix). The results are shown in Figures 11 and 12 as a function of T. The fundamental parameters used to evaluate the χ-parameters are summarized in the Appendix. It is clearly shown that, at $T > T_{MF}$, χ increases linearly with $1/T$ but the increase of χ tends to level off at $T < T_{MF}$. We wish to emphasize that this crossover temperature T_{MF}, defined *approximately and operationally*, was determined from the temperature dependencies of all the characteristic parameters I_m^{-1}, σ_q^2, and D. The leveling off in χ at $T < T_{MF}$ is parallel to the deviation from the mean-field behavior: the thermal fluctuation effect in a real system tends to make the amplitude of the concentration fluctuations smaller than that predicted by the mean-field theory. If we renormalize the effect of the thermal fluctuations on $I(q)$, as proposed by Fredrickson and Helfand,[11] we recover higher values of χ at $T < T_{MF}$ so that the renormalized χ vs $1/T$ obeys closely a linear relationship.[25] Unfortunately, however, the Fredrickson–Helfand theory cannot be applied to such low molecular weight block copolymers as those employed here. The leveling off in the increase of χ with $1/T$, as determined by the scattering methods, was reported by a few research groups.[8,17,26,27] Lin et al.[27] applied the Fredrickson–Helfand fluctuation correction[11] to the χ-values and showed in fact that the corrected χ-values change linearly with $1/T$. However, almost no works clearly related to nonlinear increase of χ to the crossover phenomenon from the mean-field behavior to the non-mean-field behavior as clarified from the relationships of both I_m^{-1} vs T^{-1} and D vs T^{-1}.

We wish to emphasize that, at $T > T_{MF}$, the scattering behavior can be described, at least to a good approximation, by Leibler's mean-field theory. Thus the χ-values should be estimated from the theoretical analysis of the scattering profiles at $T > T_{MF}$, because the fluctuation correction for low molecular weight block copolymers such as those used in this work is not available at present. The χ-values thus estimated are still subject to some errors due to residual fluctuation effects, but the errors involved should be much less than those in the χ-values determined in the temperature range of $T < T_{MF}$. The fluctuation correction at $T > T_{MF}$ is much less than that at $T < T_{MF}$. Figure 15 compares the temperature dependencies of the χ-values for OSI-1 and OSI-3 on the same graph where the arrows indicate T_{MF}. The linear part of χ vs $1/T$ at $T > T_{MF}$ is expressed by

$$\chi = -0.0237 + 34.1/T \quad (16)$$

for OSI-1 and

$$\chi = -0.0197 + 34.1/T \quad (17)$$

for OSI-3. The enthalpic part (or the slope of the plot) is about the same, but the entropic part (or the temperature-independent part) tends to decrease with increasing N.

F. Scaling of σ_q^2, I_m^{-1}, and D with χN. We will discuss the scaling behaviors of σ_q^2, I_m^{-1}, and D for

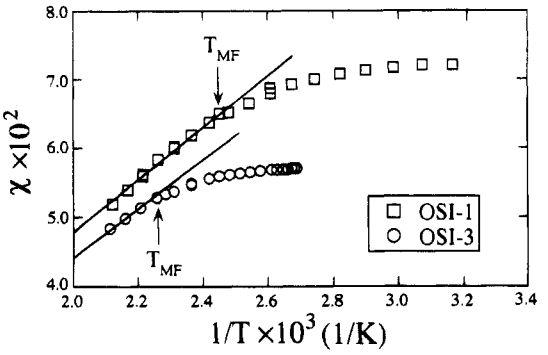

Figure 15. Comparison of the temperature dependencies of χ for OSI-1 and OSI-3.

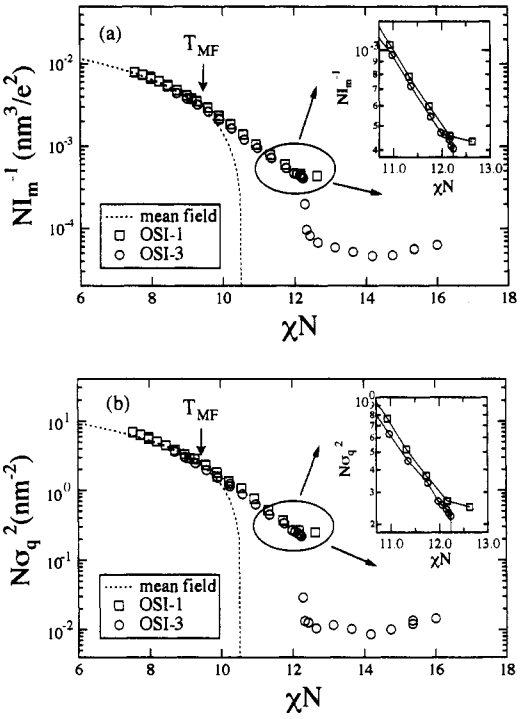

Figure 16. log NI_m^{-1} (a) and log $N\sigma_q^2$ (b) plotted against χN for OSI-1 and OSI-3. The dotted lines show the mean-field behavior.

OSI-1 and OSI-3 with χN by using the χ-values by eqs 16 and 17. From eqs 6 and 7, in the mean-field regime of $\chi N \leq (\chi N)_{MF}$, both $N\sigma_q^2$ and NI_m^{-1} should be decreasing functions which depend only χN. Figure 16 shows plots of NI_m^{-1} (a) and $N\sigma_q^2$ (b) as a function of χN for OSI-1 and OSI-3. The mean-field behaviors for NI_m^{-1} and $N\sigma_q^2$ are also shown in the figure by the dotted lines. In the mean-field regime of $T > T_{MF}$, the two sets of data obtained from OSI-1 and OSI-3 are superposed, yielding $(\chi N)_{MF} \cong 9.3$, a χN value below which the mean-field theory is applicable to the systems. The value $(\chi N)_{MF}$ was obtained from Figures 5, 8, 11, 12, and 15. The two sets of data should increasingly split with $1/T$ in the non-mean-field regime, according to the fluctuation effect elaborated by Fredrickson and Helfand;[11] i.e., NI_m^{-1} at ODT depends on N

$$NI_m^{-1} \sim N^{-1/3} \quad (18)$$

and $(\chi N)_{ODT}$ depends also on N

$$(\chi N)_{ODT} = (\chi N)_s + 41N^{-1/3} \quad (19)$$

although the tendency is not clearly discerned with this scale for the two block copolymers having only a small difference in their molecular weights.

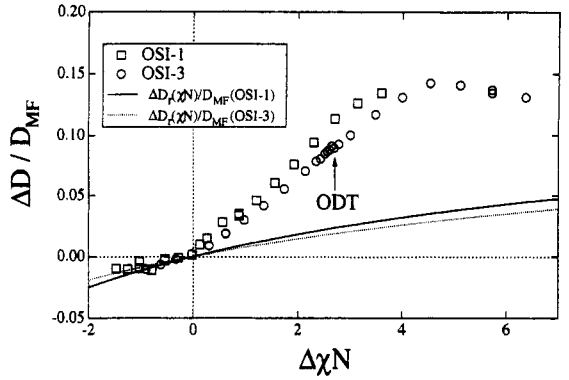

Figure 17. Plots of $\Delta D/D_{MF}$ and $\Delta D_r/D_{MF}$ (solid and dotted lines) as a function of $\Delta\chi N$ for OSI-1 and OSI-3. The arrow indicates $\Delta(\chi N)_{ODT}$ for OSI-3.

Figure 17 shows replots of $\Delta D/D_{MF}$ for OSI-1 and OSI-3 against $(\Delta\chi)N \equiv \Delta(\chi N) \equiv \chi N - (\chi N)_{MF} = BN\Delta(1/T)$, where the arrow indicates the location of the ODT for OSI-3 and the solid line and the dotted line indicate $\Delta D_r(\chi N)/D_{MF}$ of OSI-3 and OSI-1, respectively. We found $\Delta(\chi N)_{ODT} = (\chi N)_{ODT} - (\chi N)_{MF} \cong 3$ with $(\chi N)_{ODT} \cong 12.5$ for OSI-3.

V. Summary

The order–disorder transition for nearly symmetric polystyrene-*block*-polyisoprene diblock copolymers with low molecular weights was investigated by using high-temperature-resolution SAXS experiments. The results indicated the existence of two characteristic temperatures, i.e., the order–disorder transition temperature T_{ODT} and the crossover temperature T_{MF} in the disordered state; above and below T_{MF} the relevant concentration fluctuations have characteristics of the mean-field type and non-mean-field type, respectively. The characteristic parameters I_m^{-1} and D change with $1/T$ as schematically shown in Figure 1c and as described in detail in the text. The temperature dependence of the square of the half-width at half-maximum of the first-order peak in the structure factor σ_q^2 is found to be similar to that of I_m^{-1}. The χ-values estimated by matching the experimental scattering profiles at $T > T_{MF}$ and theoretical scattering function of Leibler are expressed by eqs 16 and 17 for OSI-3 and OSI-1, respectively. The higher order maxima in the structure factor exist below T_{ODT} but disappear above T_{ODT}.

Appendix

Here we summarize the scattering function $I(q)$ from the disordered melt of an A–B diblock copolymer with a polydispersity in molecular weight and an asymmetry in segmental volume. The details are given in ref 22.

$$I(q) = K'[\bar{S}(q)/\bar{W}(q) - 2\chi]^{-1} \quad \text{(A1)}$$

where K' is a proportionality constant which is not important in the present work and χ is defined in the text.

$$\bar{S}(q) = \langle S_{AA}(q)\rangle_v + 2\langle S_{AB}(q)\rangle_v + \langle S_{BB}(q)\rangle_v \quad \text{(A2)}$$

$$\bar{W}(q) = \langle S_{AA}(q)\rangle_v\langle S_{BB}(q)\rangle_v - \langle S_{AB}(q)\rangle_v^2 \quad \text{(A3)}$$

$$\langle S_{AA}(q)\rangle_v = r_{c,n}f_{A,n}^2 g_{A,n}^{(2)}(q) \quad \text{(A4)}$$

$$\langle S_{BB}(q)\rangle_v = r_{c,n}f_{B,n}^2 g_{B,n}^{(2)}(q) \quad \text{(A5)}$$

Table 3. Characteristic Parameters Used To Evaluate χ-Values

sample	W_s	$N_{S,n}$[a]	$N_{I,n}$[a]	λ	$r_{c,n}$
OSI-1	0.56	60	85	1.04	143
OSI-3	0.47	67	118	1.04	180

[a] $N_{S,n}$ and $N_{I,n}$ are number-average degree of polymerizations of polystyrene and polyisoprene block chains, respectively.

$$\langle S_{AB}(q)\rangle_v = r_{c,n}f_{A,n}f_{B,n}g_{A,n}^{(1)}(q)g_{B,n}^{(1)}(q) \quad \text{(A6)}$$

$$r_{c,n} = (v_A/v_0)N_{A,n} + (v_B/v_0)N_{B,n} \quad \text{(A7)}$$

$$v_0 = (v_A v_B)^{1/2} \quad \text{(A8)}$$

$$g_{K,n}^{(1)}(q) = \frac{1}{x_{K,n}}\{1 - [x_{K,n}(\lambda_K - 1) + 1]^{-(\lambda_K - 1)^{-1}}\} \quad \text{(A9)}$$

$$g_{K,n}^{(2)} = \frac{2}{x_{K,n}^2}\{-1 + x_{K,n} + [x_{K,n}(\lambda_K - 1) + 1]^{-(\lambda_K - 1)^{-1}}\} \quad \text{(A10)}$$

where K = A or B hereafter.

$$x_{K,n} \equiv (N_{K,n}b_K^2/6)q^2 \quad \text{(A11)}$$

$$\lambda_K = N_{K,w}/N_{K,n} \quad \text{(A12)}$$

$$f_{K,n} = N_{K,n}v_K/(N_{A,n}v_A + N_{B,n}v_B) \quad \text{(A13)}$$

In eq A7, v_K is the molecular volume of the Kth monomer, and $N_{K,n}$ is the number-average degree of polymerization of the Kth block chain. b_K in eq A11 is the segment length of the Kth chain, and $N_{K,w}$ in eq A12 is the weight-average degree of polymerization of the Kth chain. In this work we assumed $\lambda_A = \lambda_B \equiv \lambda$. In this case λ can be estimated from M_w/M_n for the block copolymer chains as a whole,

$$\lambda = [(M_w/M_n - 1)/(w_A^2 + w_B^2)] + 1 \quad \text{(A14)}$$

where $w_A = 1 - w_B$ is the weight fraction of the A block chain in the A–B block copolymer.

We used the following parameters in order to evaluate the χ-values for OSI-1 and OSI-3: $v_S = 100$ cm^3/mol and $v_I = 74.5$ cm^3/mol, where the subscripts S and I hereafter stand for polystyrene and polyisoprene block chains, respectively. Other parameters used are summarized in Table 3. Here we used b_S and b_I as floating parameters to fit the experimental and theoretical peak scattering vector q_m. χ was determined as a value which gives rise to a best fit between the experimental and theoretical relative intensity distributions.

References and Notes

(1) Leibler, L. *Macromolecules* **1980**, *13*, 1602.
(2) Hashimoto, T.; Tsukahara, Y.; Kawai, H. *J. Polym. Sci., Polym. Lett. Ed.* **1980**, *18*, 585; *Macromolecules* **1981**, *14*, 708.
(3) Roe, R. J.; Fishkis, M.; Chang, J. C. *Macromolecules* **1981**, *14*, 1091.
(4) Hashimoto, T.; Shibayama, M.; Kawai, H. *Macromolecules* **1983**, *16*, 1093.
(5) Zin, W. C.; Roe, R. J. *Macromolecules* **1984**, *17*, 183.
(6) Mori, K.; Hasegawa, H.; Hashimoto, T. *Polym. J.* **1985**, *17*, 799.
(7) Bates, F. S.; Hartney, M. A. *Macromolecules* **1985**, *18*, 2478.
(8) Hashimoto, T.; Ijichi, Y.; Fetters, L. J. *J. Chem. Phys.* **1988**, *89*, 2463. Ijichi, Y.; Hashimoto, T.; Fetters, L. J. *Macromolecules* **1989**, *22*, 2817.
(9) Owens, J. N.; Gancarz, I. S.; Koberstein, J. T.; Russell, T. P. *Macromolecules* **1989**, *22*, 3380.

(10) Bates, F. S.; Rosedale, J. H.; Fredrickson, G. H. *J. Chem. Phys.* **1990**, *92*, 6255.
(11) Fredrickson, G. H.; Helfand, E. *J. Chem. Phys.* **1987**, *87*, 697.
(12) Brazovskii, A. *Sov. Phys.—JETP (Engl. Transl.)* **1975**, *41*, 85.
(13) Bates, F. S.; Wilzius, P. *J. Chem. Phys.* **1989**, *91*, 3258.
(14) Stühn, B.; Mutter, R.; Albrecht, T. *Europhys. Lett.* **1992**, *18*, 427.
(15) Wolff, T.; Burger, C.; Ruland, W. *Macromolecules* **1993**, *26*, 1707.
(16) Hashimoto, T.; Ogawa, T.; Han, C. D. *J. Phys. Soc. Jpn.* **1994**, *63*, 2206.
(17) Floudas, G.; Pakula, T.; Fischer, E. W.; Hadjichristidis, N.; Pispas, S. *Acta Polym.* **1994**, *45*, 176.
(18) Winey, K. I.; Gobran, D. A.; Xu, Z.; Fetters, L. J.; Thomas, E. L. *Macromolecules* **1994**, *27*, 2392.
(19) Rosedale, J. H.; Bates, F. S.; Almdal, K.; Mortensen, K.; Wignall, D. *Macromolecules* **1995**, *28*, 1429.
(20) Hashimoto, T.; Suehiro, S.; Shibayama, M.; Saijo, K.; Kawai, H. *Polym. J.* **1981**, *13*, 501. Fujimura, M.; Hashimoto, T.; Kawai, H. *Mem. Fac. Eng., Kyoto Univ.* **1981**, *43* (2), 224. Suehiro, S.; Saijo, K.; Ohta, Y.; Hashimoto, T.; Kawai, H. *Anal. Chim. Acta* **1986**, *189*, 41.
(21) Mays, J. W.; Hadjichristidis, N.; Fetters, L. J. *Macromolecules* **1985**, *18*, 2231.
(22) Sakurai, S.; Mori, K.; Okawara, A.; Kimishima, K.; Hashimoto, T. *Macromolecules* **1992**, *25*, 2679.
(23) Muthukumar, M. *Macromolecules* **1993**, *26*, 5259.
(24) Barret, J.-L.; Fredrickson, G. H. *J. Chem. Phys.* **1991**, *95*, 1281.
(25) Inoue, T.; Hashimoto, T., unpublished results.
(26) Holzer, B.; Lehman, A.; Stühn, B.; Kowalski, M. *Polymer* **1991**, *32*, 1935.
(27) Lin, C. C.; Jonnalagadda, S. V.; Kesani, P. K.; Dai, H. J.; Balsara, N. P. *Macromolecules* **1994**, *27*, 7769.

MA9502359